Journal of Sound and Vibration (1998) **216**(2), 281–294
Article No. sv981662

BOUNDARY INTEGRAL EQUATION METHOD FOR EVALUATING THE PERFORMANCE OF STRAIGHT-THROUGH RESONATOR WITH MEAN FLOW

C.-N. Wang and C.-Y. Liao
Department of Naval Architecture and Ocean Engineering, National Taiwan University, Taipei, Taiwan, Republic of China

(*Received* 13 *November* 1997, *and in final form* 19 *March* 1998)

In this paper, a numerical scheme for modelling the straight-through resonator with mean flow based upon the boundary integral equation method is developed. The approach can be applied to both short and long resonators with perforated center tube, and the results agree well with the experimental measurements reported in the literature without mean flow. The two effects, i.e., the convection effect, and the change in acoustic impedance of the perforated tube and of mean flow velocity on the acoustic performance of a straight-through resonator, are both considered. Further, other parameters such as porosity, tube thickness, and hole diameter are also investigated.

1. INTRODUCTION

The resonator is a widely used component in the contemporary automotive exhaust system. The effect of the perforated center tube in the concentric-tube resonator is to regulate the mean flow and also increase the silencing performance. In the past, the analysis of concentric-tube resonator has been performed by the Helmholtz resonator theory [1], which can treat a low frequency and low porosity resonator well. But it is not suitable for a resonator with a long perforated tube or a high porosity tube. Further, the flow velocity is also not included. In 1978, Sullivan and Crocker [2, 3] initially derived the coupled equations of sound propagation in the perforated center tube and the outer cavity. They obtained a close form solution but the resonator configuration should have been acoustically long in one direction. Later, under the assumption of plane wave propagation, Jayaraman and Yam [4] and Thawani and Jayaraman [5] proposed a decoupling method for the coupled equations derived by Sullivan and Crocker. In order to decouple the equations, they assumed that the mean flow velocities in the center tube and the outer cavity are the same which is contrary to the physical law. Munjal *et al*. [6] and Peat [7] also broached the generalized decoupling method and numerical decoupling method respectively to solve the coupling equations. All the methods mentioned above are based upon the assumption of plane wave propagation. Wang [8] proposed a boundary element approach to extend to a higher order mode and complex boundary surface analysis. The convection effect of mean flow on the performance of a resonator, however, is not included.

In the present work, a boundary element method to analyze the concentric-tube resonator with mean flow is developed. The four-pole parameters evaluated by the present method can be used to predict the acoustic performance of a resonator. The influences of mean flow, including the convection effect and the change on acoustic impedance of the perforated tube, are taken into consideration. Further, the effects of the porosity, tube thickness and the hole diameter are also investigated.

2. GOVERNING EQUATIONS

The straight-through resonator considered is shown in Figure 1. To simplify the numerical process, the resonator is considered to be made up of two acoustic control volumes; one is the center tube and the other is the outer cavity. The two control volumes couple with each other via the perforated surface. From Sullivan's experiment [9], it can be understood that most of the medium flows straight through the center tube and only a little mass flows into the outer cavity at the fore stage of the perforated surface and flows out at the end part. It is, therefore, assumed in the present study that the mean flow only exists in the centre tube.

The velocity potential Φ of the acoustic wave propagated in the two control volumes should be governed by

$$\nabla^2\Phi^I - \frac{1}{c^2}\left(\frac{\partial}{\partial t} + \mathbf{V}\cdot\nabla\right)^2\Phi^I = 0 \qquad \text{in the center tube} \tag{1}$$

and

$$\nabla^2\Phi^{II} - \frac{1}{c^2}\frac{\partial\Phi^{II}}{\partial t^2} = 0 \qquad \text{in the outer cavity,} \tag{2}$$

where $\mathbf{V}$ is the mean flow velocity and c is the sound speed in the stationary medium. Assume that sound propagation is a harmonic motion ($e^{i\omega t}$) and also the mean flow velocity is in the x direction. Then equations (1) and (2) can be rewritten as

$$\nabla^2\phi^I + k^2\phi^I - 2ikM\frac{\partial\phi^I}{\partial x} - M^2\frac{\partial^2\phi^I}{\partial x^2} = 0 \tag{3}$$

and

$$\nabla^2\phi^{II} + k^2\phi^{II} = 0, \tag{4}$$

where $k = \omega/c$ is the wave number, ω is the angular frequency, and $M = |\mathbf{V}|/c$ is the mean flow Mach number. ϕ^I and ϕ^{II}, dependent on the space only, denote the acoustic velocity

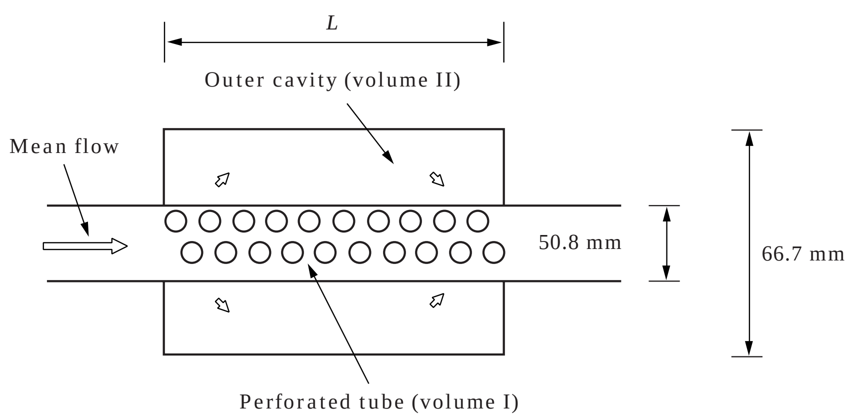

Figure 1. The configuration of the straight-through resonator. Long resonator $L = 257{\cdot}2$ mm; short resonator $h = 66{\cdot}7$ mm.

potential amplitudes in the center tube and the outer cavity, respectively. The complex equation (3) is transformed into a Helmholtz equation in order that the numerical implementation for the Helmholtz equation can be applied to equations (3) and (4) directly. By applying the Prandtl–Glauert transformation [10]

$$\tilde{x} = \frac{x}{\sqrt{1 - M^2}}, \qquad \tilde{y} = y, \qquad \tilde{z} = z \tag{5}$$

and $\tilde{\phi}^I = \phi^I \, \mathrm{e}^{-\mathrm{i}\hbar\tilde{x}}$, equation (3) is converted to a Helmholtz equation and is expressed as

$$\tilde{\nabla}^2 \tilde{\phi}^I + \tilde{k}^2 \tilde{\phi}^I = 0, \tag{6}$$

where

$$\hbar = \frac{kM}{\sqrt{1 - M^2}} \qquad \text{and} \qquad \tilde{k} = \frac{\hbar}{M}.$$

Equations (4) and (6) are the governing equations for the sound propagation in a straight-through resonator with mean flow.

3. NUMERICAL IMPLEMENTATION

In order to transform the differential equations into the boundary integral equations, the Green second identity and Gauss theorem are applied to the Helmholtz equation and their adjoint obtains

$$C(\beta)\phi(\beta) = \int_S \left[G(\alpha, \beta) \frac{\partial \phi}{\partial \mathbf{n}}(\alpha) - \frac{\partial G(\alpha, \beta)}{\partial \mathbf{n}(\alpha)} \phi(\alpha) \right] \mathrm{d}S(\alpha), \tag{7}$$

where S is the surface of the acoustical control volume and $\mathbf{n}$ denotes the unit outward normal vector. G is the fundamental solution of the non-homogeneous Helmholtz equation and is expressed as

$$G(\alpha, \beta) = \frac{\mathrm{e}^{-\mathrm{i}\kappa r(\alpha,\beta)}}{r(\alpha, \beta)}, \tag{8}$$

where κ represents the wave number in the Helmholtz equation and r is the distance between the points of α and β. The coefficient $C(\beta)$ is the solid angle at point β and can be expressed as [11]

$$C(\beta) = -\int_S \frac{\partial}{\partial \mathbf{n}(\alpha)} \left(\frac{1}{r(\alpha, \beta)} \right) \mathrm{d}S(\alpha). \tag{9}$$

By applying the processes mentioned above to equations (4) and (6), two Helmholtz boundary integral equations, the same as that of equation (7), are obtained. To regularize the singularity of integration when the point α approaches β, the method used in reference [11] is also adopted in the present study. The boundary surface of each control volume is divided into two parts, where ΔS is a small region which contains the point β, and S_o denotes the remaining surface. If a strong singularity term

$$\phi(\beta) \int_{\Delta S} \frac{\partial}{\partial \mathbf{n}(\alpha)} \left(\frac{\mathrm{e}^{-\mathrm{i}\kappa r(\alpha,\beta)}}{r(\alpha, \beta)} \right) \mathrm{d}S(\alpha) \tag{10}$$

is added to both sides of the Helmholtz integral equation, the boundary integral equations for the transformed center tube and outer cavity can be written as

$$-\phi^j(\beta)\int_{S_o^j}\frac{\partial}{\partial\mathbf{n}(\alpha)}\left[\frac{1}{r(\alpha,\beta)}\right]\mathrm{d}S(\alpha)+\int_{S_o^j}\phi^j(\alpha)\frac{\partial}{\partial\mathbf{n}(\alpha)}\left[\frac{\mathrm{e}^{-\mathrm{i}\kappa r(\alpha,\beta)}}{r(\alpha,\beta)}\right]\mathrm{d}S(\alpha)$$

$$+\phi^j(\beta)\int_{\Delta S^j}\left\{\frac{\partial}{\partial\mathbf{n}(\alpha)}\left[\frac{\mathrm{e}^{-\mathrm{i}\kappa r(\alpha,\beta)}}{r(\alpha,\beta)}\right]-\frac{\partial}{\partial\mathbf{n}(\alpha)}\left[\frac{1}{r(\alpha,\beta)}\right]\right\}\mathrm{d}S(\alpha)$$

$$+\int_{\Delta S^j}\frac{\partial}{\partial\mathbf{n}(\alpha)}\left[\frac{\mathrm{e}^{-\mathrm{i}\kappa r(\alpha,\beta)}}{r(\alpha,\beta)}\right][\phi^j(\alpha)-\phi^j(\beta)]\,\mathrm{d}S(\alpha)$$

$$=\int_{S_o^j}\frac{\partial\phi^j}{\partial n}(\alpha)\left[\frac{\mathrm{e}^{-\mathrm{i}\kappa r(\alpha,\beta)}}{r(\alpha,\beta)}\right]\mathrm{d}S(\alpha)+\int_{\Delta S^j}\frac{\partial\phi^j}{\partial n}(\alpha)\left[\frac{\mathrm{e}^{-\mathrm{i}\kappa r(\alpha,\beta)}}{r(\alpha,\beta)}\right]\mathrm{d}S(\alpha)$$

$$j=I,II. \tag{11}$$

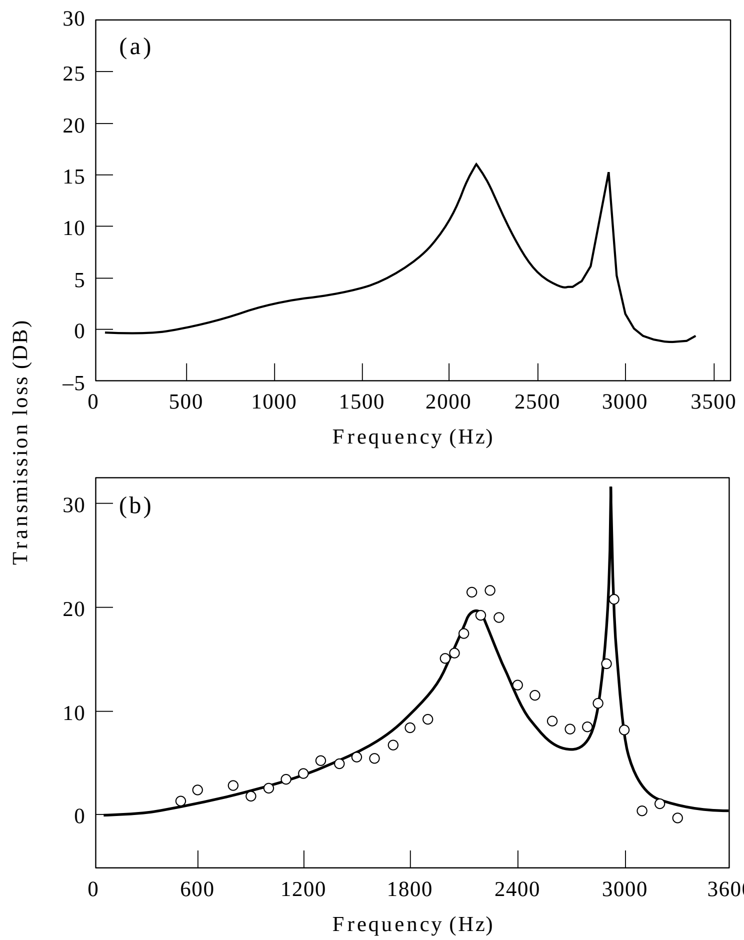

Figure 2. Comparison of the transmission loss of a short resonator without mean flow. (a) Present method. (b) Results of reference [2]: cavity length = 66·7 mm; cavity O.D. = 76·2 mm; cavity I.D. = 50·8 mm; porosity = 3·7%.

The quantities, such as the velocity potential ϕ^j, the wave number κ, the outward unit normal vector $\mathbf{n}$, and the distance r, in equation (11) represent $\tilde{\phi}^I$, $\tilde{k}$, $\tilde{n}$, $\tilde{r}$ on the center tube transformed domain for $j = I$ and denote ϕ^{II}, k, n, r on the outer cavity for $j = II$, respectively. The integration of the weak singularity, the second term on the right side can be treated by a polar co-ordinate transformation.

By performing the numerical integration on the discretized elements of $\tilde{S}^I$, the surface of the transformed center tube, and of S^{II}, the surface of outer cavity, the velocity potential and its gradient on the boundary can be related by

$$[\tilde{A}]^I\{\tilde{\phi}\}^I = [\tilde{B}]^I\left\{\frac{\partial\tilde{\phi}}{\partial\tilde{\mathbf{n}}}\right\}^I \qquad \text{for the transformed center tube} \tag{12}$$

and

$$[A]^{II}\{\phi\}^{II} = [B]^{II}\left\{\frac{\partial\phi}{\partial\mathbf{n}}\right\}^{II} \qquad \text{for the outer cavity.} \tag{13}$$

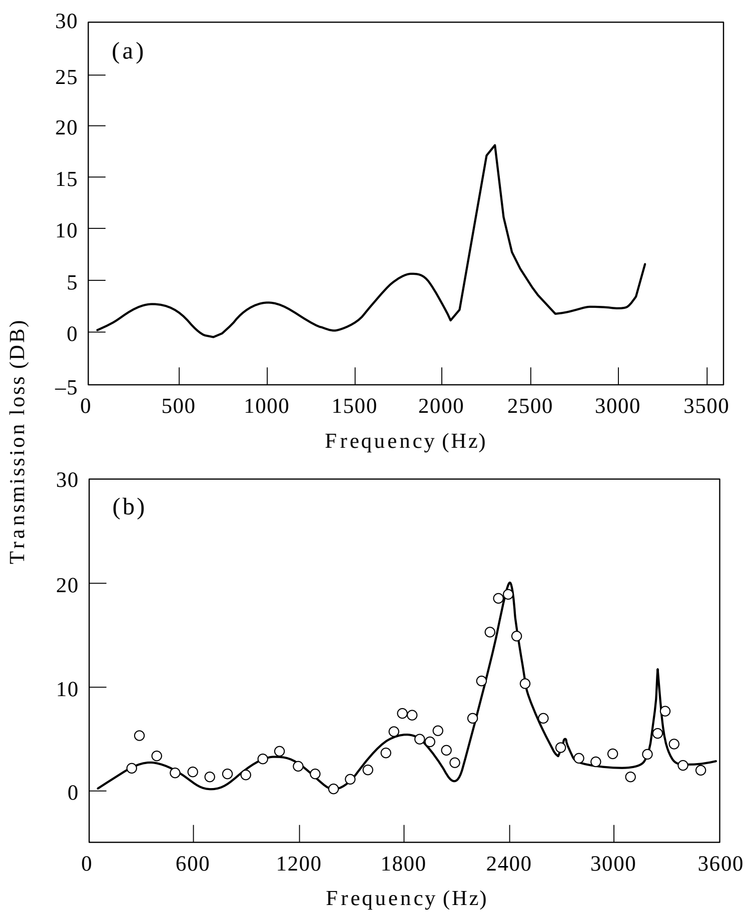

Figure 3. Comparison of the transmission loss of a long resonator without mean flow. (a) Present method. (b) Results of reference [2]: cavity length = 257·2 mm; cavity O.D. = 76·2 mm; cavity I.D. = 50·8 mm; porosity = 3·8%.

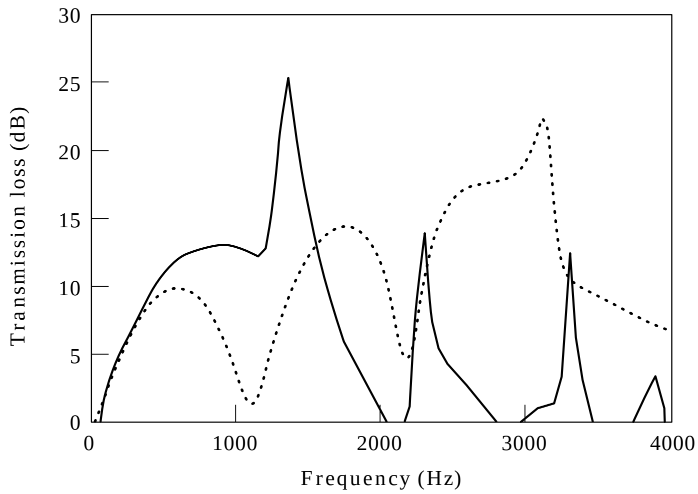

Figure 4. Comparison of results of the plane wave theory (----) and the present method (——) for the performance of a resonator with mean flow velocity $M = 0{\cdot}05$.

With the following relations

$$\tilde{\phi}^I = \phi^I \, \mathrm{e}^{-\mathrm{i}\hbar \tilde{x}}, \qquad \frac{\partial \tilde{\phi}^I}{\partial \tilde{\mathbf{n}}} = \mathrm{e}^{-\mathrm{i}\hbar \tilde{x}} \left(\frac{\partial \phi^I}{\partial \mathbf{n}} \frac{\partial \mathbf{n}}{\partial \tilde{\mathbf{n}}} - \mathrm{i}\hbar \phi^I \tilde{\mathbf{n}}_x \right), \tag{14, 15}$$

equation (12) can be converted to the real physical domain and is expressed as

$$[A]^I \{\phi\}^I = [B]^I \left\{ \frac{\partial \phi}{\partial \mathbf{n}} \right\}^I \qquad \text{for the center tube,} \tag{16}$$

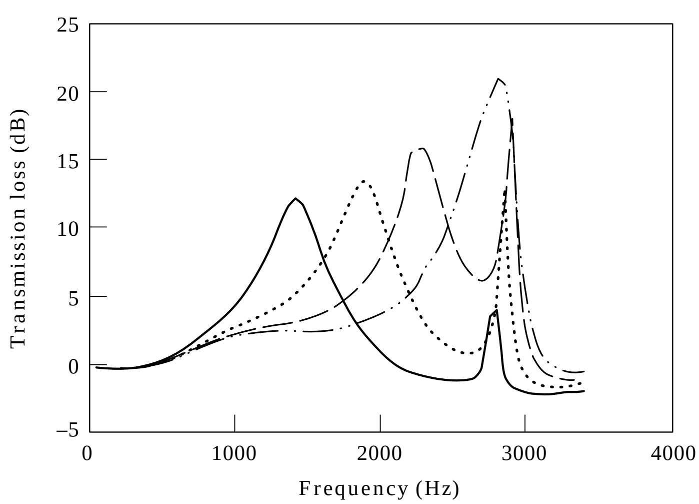

Figure 5. The effect of porosity on the transmission loss for a short resonator without mean flow: ——, $\sigma = 0{\cdot}02$; - - -, $\sigma = 0{\cdot}03$; — —, $\sigma = 0{\cdot}04$; -·-·-, $\sigma = 0{\cdot}05$.

where $A^I_{\ell m} = \tilde{A}^I_{\ell m}\,\mathrm{e}^{-\mathrm{i}h\tilde{x}} + \tilde{B}^I_{\ell m}\,\mathrm{e}^{-\mathrm{i}h\tilde{x}}\mathrm{i}\hbar(\tilde{\mathbf{n}}_x)_m$, and $B^I_{\ell m} = \tilde{B}^I_{\ell m}\,\mathrm{e}^{-\mathrm{i}h\tilde{x}_m}\,\partial\mathbf{n}_m/\partial\tilde{\mathbf{n}}_m$. To evaluate the performance of a resonator, the velocity potential and its gradient should be converted to pressure and normal velocity initially by

$$p = \rho_0(\mathrm{i}\omega\phi) + \rho_0 V\frac{\partial\phi}{\partial x}, \tag{17}$$

and

$$u_n = -\frac{\partial\phi}{\partial\mathbf{n}} \tag{18}$$

Therefore, equations (13) and (16) are rewritten as

$$[H]^I\{p\}^I = [G]^I\{\rho_0 c u_n\}^I, \qquad [H]^{II}\{p\}^{II} = [G]^{II}\{\rho_0 c u_n\}^{II}, \tag{19, 20}$$

where

$$\begin{cases} H^I_{ij} = A^I_{ij} \\ G^I_{ij} = (-\mathrm{i}k)B^I_{ij} - A^I_{ij}M\cos(\mathbf{n}, x)^I_j \\ H^{II}_{ij} = A^{II}_{ij} \\ G^{II}_{ij} = (-\mathrm{i}k)B^{II}_{ij} \end{cases}.$$

Since the center tube and the outer cavity are coupled to each other via the common perforated surface, equations (19) and (20) must be solved simultaneously. Suppose the nodal points on the center tube are divided into three groups, group 1: nodes on the inlet and the outlet, group 2: nodes on the common perforated surface, and group 3: nodes on all of the remaining surface. Similarly, the nodes on the outer cavity are partitioned into two parts, one includes the nodes on the common surface and the other contains all of the remaining nodes. Therefore, equations (19) and (20) become

$$\begin{bmatrix} H_{11} & H_{12} & H_{13} \\ H_{21} & H_{22} & H_{23} \\ H_{31} & H_{32} & H_{33} \end{bmatrix}^I \begin{Bmatrix} p_{in,out} \\ p_c \\ p_{other} \end{Bmatrix}^I = \begin{bmatrix} G_{11} & G_{12} & G_{13} \\ G_{21} & G_{22} & G_{23} \\ G_{31} & G_{32} & G_{33} \end{bmatrix}^I \begin{Bmatrix} \rho_0 c u_{nin,out} \\ \rho_0 c u_{nc} \\ \rho_0 c u_{nother} \end{Bmatrix}^I, \tag{21}$$

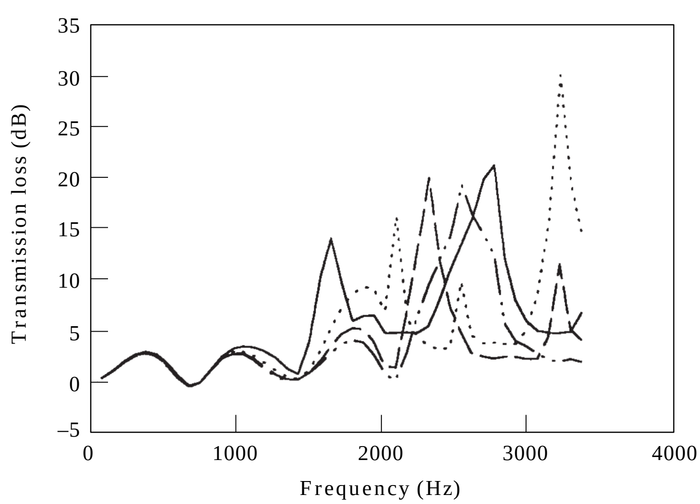

Figure 6. The effects of porosity on the transmission loss for a long resonator without mean flow. Key same as Figure 5.

$$\begin{bmatrix} H_{11} & H_{12} \\ H_{21} & H_{22} \end{bmatrix}^{II} \begin{Bmatrix} p_c \\ p_{other} \end{Bmatrix}^{II} = \begin{bmatrix} G_{11} & G_{12} \\ G_{21} & G_{22} \end{bmatrix}^{II} \begin{Bmatrix} \rho_0 c u_{nc} \\ \rho_0 c u_{nother} \end{Bmatrix}^{II}. \tag{22}$$

The perforated surface is equivalent to an acoustic impedance surface and the boundary conditions on this surface can be expressed as

$$u^I_{nc} = (p^I_c - p^{II}_c)/\rho_0 c\xi, \qquad u^{II}_{nc} = (p^{II}_c - p^I_c)/\rho_0 c\xi, \tag{23, 24}$$

where $\rho_0 c$ is the characteristic impedance of the medium and ξ is the specific acoustic impedance. Further, the other parts of the wall of the resonator are assumed to be hard, i.e.,

$$u_{nother} = 0. \tag{25}$$

Substituting equations (24) and (25) into equation (22) and eliminating the term $\{p_{other}\}^{II}$ gives the relationship between $\{p_c\}^I$ and $\{p_c\}^{II}$ and is expressed as

$$\{p_c\}^{II} = [TR]\{p_c\}^I, \tag{26}$$

where

$$[TR] = [H^{II}_{12}(H^{II}_{22})^{-1}(H^{II}_{21} - G^{11}_{21}/\xi) - (H^{II}_{11} - G^{II}_{11}/\xi)]^{-1}[H^{II}_{12}(H^{II}_{22})^{-1}(-G^{II}_{21}/\xi) + G^{II}_{11}/\xi]. \tag{27}$$

Therefore, by means of equations (23), (25) and (26), equation (21) can be rewritten as

$$\begin{bmatrix} H^I_{11} & H^I_{12} - G^I_{12}/\xi + G^I_{12}/\xi[TR] & H^I_{13} \\ H^I_{21} & H^I_{22} - G^I_{22}/\xi + G^I_{22}/\xi[TR] & H^I_{23} \\ H^I_{31} & H^I_{32} - G^I_{32}/\xi + G^I_{32}/\xi[TR] & H^I_{33} \end{bmatrix} \begin{Bmatrix} p^I_{in,out} \\ p^I_c \\ p^I_{other} \end{Bmatrix} = \begin{bmatrix} G^I_{11} \\ G^I_{21} \\ G^I_{31} \end{bmatrix} \{\rho c u^I_{nin,out}\}. \tag{28}$$

When the boundary conditions are specified, the pressure and normal velocity distribution on the center tube can be obtained and consequently the transmission loss of the resonator can also be evaluated.

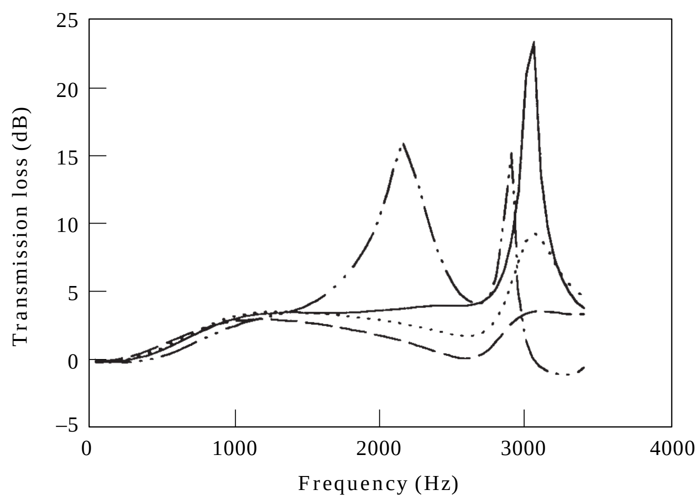

Figure 7. The effect of mean flow velocity on the transmission loss for a short straight-through resonator: ——, $M = 0{\cdot}05$; ----, $M = 0{\cdot}1$; –––, $M = 0{\cdot}2$; –·–, $M = 0$.

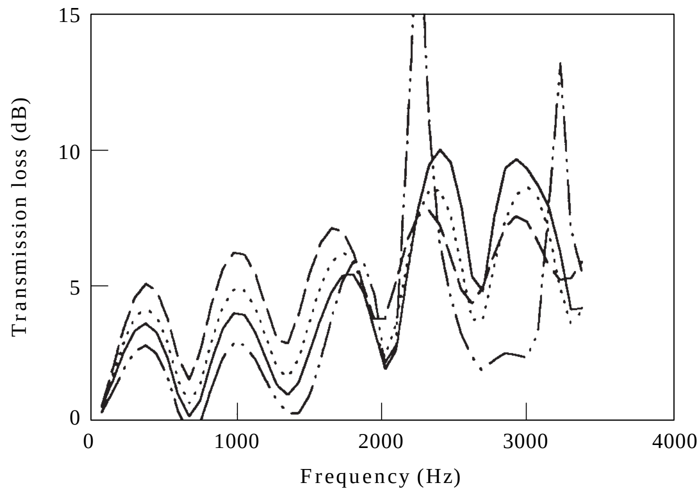

Figure 8. The effect of mean flow velocity on the transmission loss for a long straight-through resonator. Key same as Figure 7.

4. TRANSMISSION LOSS

A straight-through resonator can be regarded as a linear acoustic system with an inlet and outlet. Thus, the evaluation of the transmission loss of a resonator is the same as that of a simple expansion muffler [11]. The four-pole matrix between the inlet and the outlet of an acoustic system is expressed as

$$\begin{Bmatrix} p \\ \rho c u_n \end{Bmatrix}_{in} = \begin{bmatrix} A & B \\ C & D \end{bmatrix} \begin{Bmatrix} p \\ \rho c u_n \end{Bmatrix}_{out}, \tag{29}$$

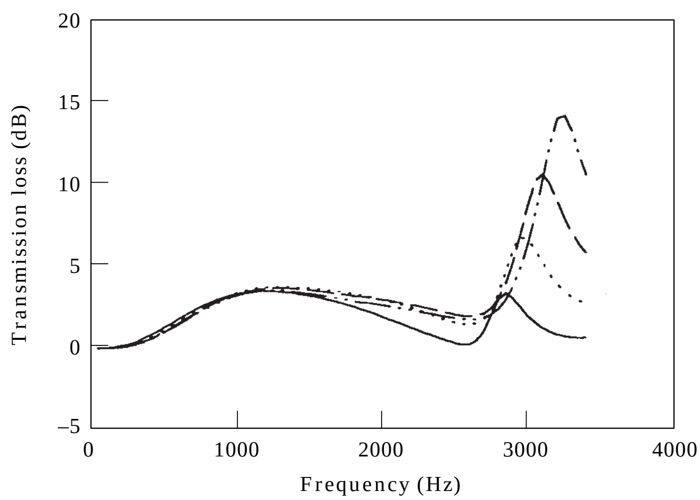

Figure 9. The effect of porosity on the transmission loss for a short resonator with mean flow velocity $M = 0{\cdot}1$: ——, $\sigma = 0{\cdot}02$; ----, $\sigma = 0{\cdot}03$; –––, $\sigma = 0{\cdot}04$; –·–·–, $\sigma = 0{\cdot}05$.

where A, B, C, D are the four-pole parameters and are obtained from

$$A = \frac{p_{in}}{p_{out}}\bigg|_{u_{nout}} = 0, \qquad B = \frac{p_{in}}{\rho c u_{nout}}\bigg|_{p_{out}} = 0 \tag{30, 31}$$

$$C = \frac{\rho c u_{nin}}{-\,p_{out}}\bigg|_{u_{nout}} = 0, \qquad D = \frac{\rho c u_{nin}}{-\,\rho c u_{nout}}\bigg|_{p_{out}} = 0. \tag{32, 33}$$

As long as the four-pole parameters are determined, the transmission loss of a straight-through resonator with mean flow can be easily obtained. Since the cross-section area of the inlet and the outlet are the same, the transmission loss is calculated by [12]

$$TL = 20\log_{10}\left(\left|\frac{A+B+C+D}{2}\right|\right). \tag{34}$$

5. ACOUSTIC IMPEDENCE OF A PERFORATED TUBE

In the present study, the center tube and the outer cavity of a resonator are regarded as an acoustical control volume individually. The only connection between these two volumes is through the drilling holes on the center tube. The characteristic of the perforated surface is equivalent to an acoustic impedance which can be determined experimentally [2, 13]. The acoustic impedance is assumed to be constant along the perforated tube since the drilling holes are uniformly distributed on the perforated surface. To simplify the effort, the empirical formulae of specific acoustic impedance proposed by Sullivan and Crocker [2] and Rao [13] for stationary media and grazing flow are used.

For the case of perforates in stationary media [2]

$$\xi = \frac{1}{\sigma}\left[6 \times 10^{-3} + \mathrm{i}k(t + 0{\cdot}75 d_h)\right], \tag{35}$$

where σ denotes the porosity, t is the thickness of the perforated tube and d_h is the hole diameter.

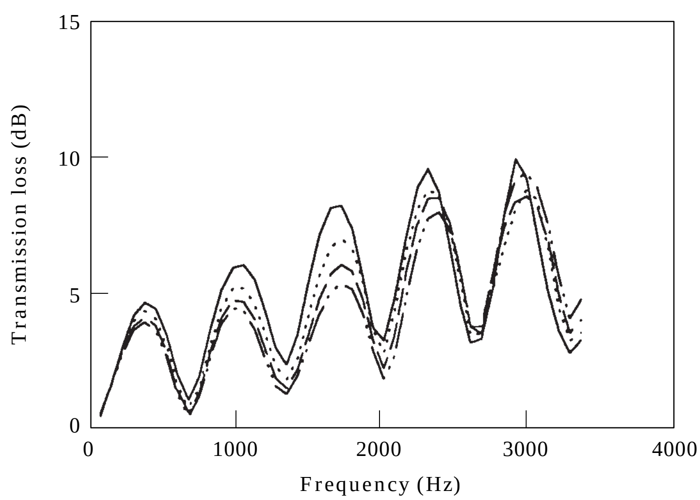

Figure 10. The effect of porosity on the transmission loss for a long resonator with mean flow velocity $M = 0{\cdot}1$. Key same as Figure 9.

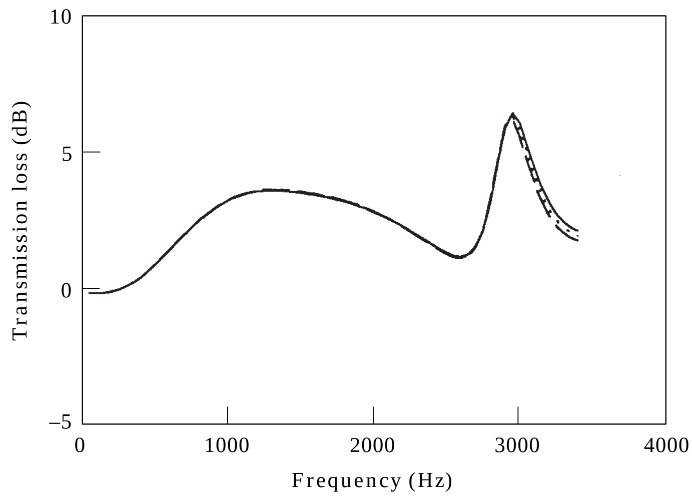

Figure 11. The effect of the tube thickness on the transmission loss for a short resonator with mean flow velocity $M = 0{\cdot}1$: ——, $t = 0{\cdot}5$ mm; ----, $t = 1{\cdot}0$ mm; −−−, $t = 1{\cdot}5$ mm.

For the case of perforates with grazing flow [3]

$$\xi = \frac{1}{\sigma}\left[7{\cdot}337 \times 10^{-3}(1 + 72{\cdot}23M) + \mathrm{i}2{\cdot}2245 \times 10^{-5}(1 + 51t)(1 + 204d_h)f\right], \qquad (36)$$

where M is the mean flow Mach number in the center tube and f is the sound frequency to be analyzed. It should be noted that t and d_h in equation (33) must be in meters (m).

6. NUMERICAL RESULTS

The dimensions of the straight through resonators to be considered are shown in Figure 1. The default values of the other parameters adopted in the present study are expressed as follows: the tube thickness is 0·81 mm; the porosity is 0·037; the diameter of the drilling hole is 2·49 mm; and the mean flow velocity is 0·1 Mach.

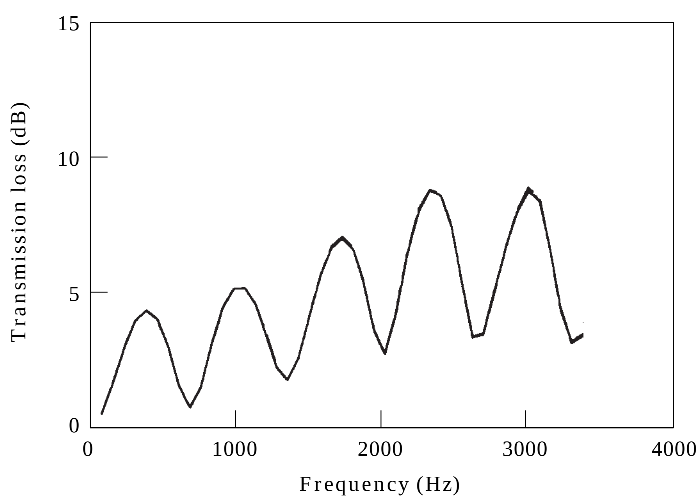

Figure 12. The effect of the tube thickness on the transmission loss for a long resonator with mean flow velocity $M = 0{\cdot}1$. Key same as Figure 11.

6.1. STRAIGHT THROUGH RESONATOR WITHOUT MEAN FLOW

Two resonators, measured by Sullivan and Crocker [2], are initially chosen for analysis in order to verify the accuracy of the present method. Figures 2 and 3 show the comparisons of the transmission loss of a short resonator (6·67 cm) and a long resonator (25·72 cm), respectively. It can be seen that the agreement is good. This confirms that the present method predicts the transmission loss of a resonator accurately. Further, the other straight-through resonator used as a component in an actual diesel engine exhaust muffler is analyzed by the plane wave theory [7] and the present method. The dimensions of this resonator are: length 16 cm, inner and outer diameters 10 and 22 cm, tube thickness 2 mm, hole diameter 3 mm and porosity 0·09818. The results obtained by these two methods are shown in Figure 4. It is seen that the plane wave model predicts a better performance in the high frequency range. However, the non-plane wave occurs at lower frequencies as that predicted by the present method and thus the performance becomes poor at higher frequencies. This phenomenon reveals that a more complicated approach than that of the plane wave model is required in predicting the performance of a resonator.

The effect of porosity for a short resonator is analyzed and shown in Figure 5. It is seen that the magnitude and the corresponding frequency of the main noise reduction peak are raised as the porosity is increased. Similar results are also found in the long resonator, as shown in Figure 6. However, the transmission loss curves become more complicated.

6.2. STRAIGHT THROUGH RESONATOR WITH MEAN FLOW

The resonators to be considered are the same as those mentioned above, long and short straight through resonators. The dimensions are shown in Figure 1. The effect of mean flow velocity on the performance of a short and a long straight-through resonator are shown in Figures 7 and 8, respectively. From these two figures it is seen that the mean flow has a strong effect on the performance of a resonator. For the short resonator, the magnitude of the main noise reduction peak is reduced obviously when the mean flow velocity increases, as shown in Figure 7. However, in Figure 8, the performance of a long resonator is increased as the mean flow velocity is increased for frequencies below about 2300 Hz, which corresponds to the frequency of the resonance peak in Figure 3. It is also

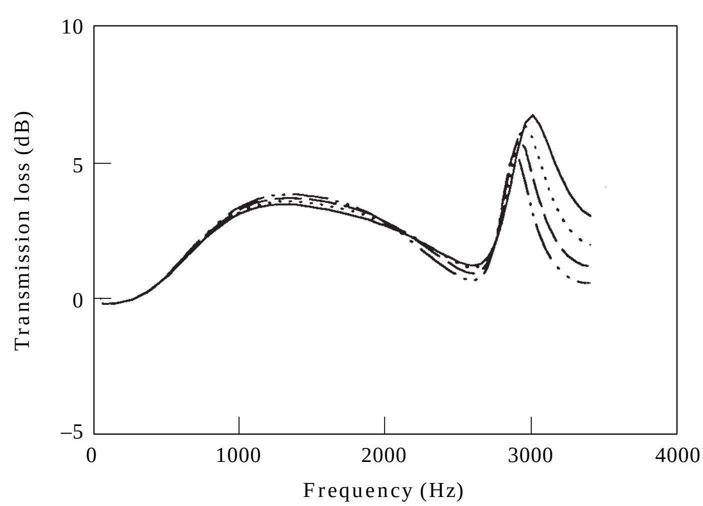

Figure 13. The effect of the hole diameter on the transmission loss for a short resonator with mean flow velocity $M = 0{\cdot}1$: ——, $d = 2$ mm; ----, $d = 3$ mm; – – –, $d = 4$ mm; –·–, $d = 5$ mm.

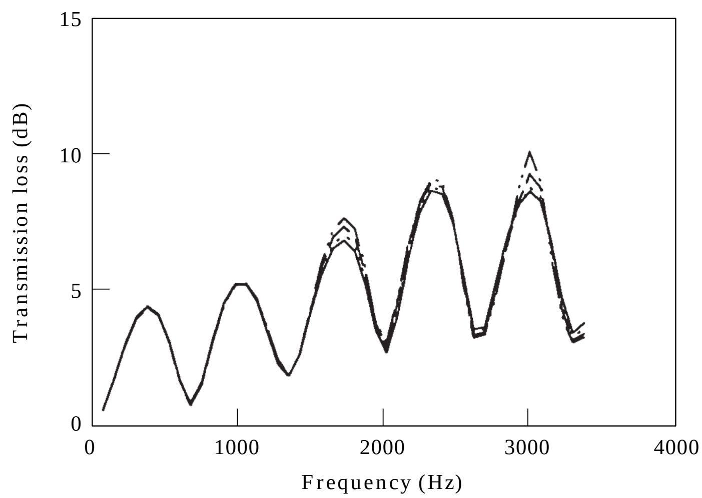

Figure 14. The effect of the hole diameter on the transmission loss for a long resonator with mean flow velocity $M = 0{\cdot}1$. Key same as Figure 13.

seen that the resonance peak at about 2300 Hz is inapparent and the performance is reduced as the mean flow velocity is increased for frequencies higher than 2300 Hz.

The other parameter to be investigated is porosity. Figure 9 shows the transmission loss curves of a short resonator with different porosities. The magnitude and the corresponding frequency of the main peak are raised as the porosity is increased. For a long resonator with mean flow, however, the main peak is not obvious and the performance is reduced as the porosity is increased in the frequency range analyzed, as shown in Figure 10. The effect of the center tube thickness is also studied. From practical consideration, only thicknesses of 0·5, 1 and 1·5 mm are analyzed. Figures 11 and 12 show the performance curves of the short and the long resonators, respectively. It is seen that the influence of the tube thickness on the transmission loss is inapparent. The final parameter studied is the diameter of the drilling hole. Figure 13 shows the transmission loss curves of a short resonator with different drilling hole diameters. The frequency and the magnitude of the main noise reduction peak are both reduced as the hole diameter is increased. But for a long straight-through resonator the performance is improved as the drilling hole diameter is increased, as shown in Figure 14.

7. CONCLUSION

A boundary element approach for a straight-through resonator with mean flow has been developed. The numerical results of a short and a long resonator without mean flow compared to those published in the literature are good. For a straight-through resonator without mean flow, the porosity is the most important parameter to affect the acoustic performance. Either for a short or for a long straight-through resonator, the frequency of occurrence of the main noise reduction peak is increased as the porosity is increased.

For a straight-through resonator with mean flow, the number of parameters to affect the acoustic performance is increased. These include mean flow velocity, porosity, tube thickness and drilling hole diameter. From the results of the numerical analysis, it can be seen that the tube thickness and the drilling hole diameter do not have a significant influence on the acoustic performance of a straight-through resonator. For a short resonator, the effects of porosity are to raise the frequency and the magnitude of the main noise reduction peak, but the extent of the influence is not as obvious as that in the case without mean flow. However, for a long resonator, the increase in porosity just reduces the performance in the desired frequency range. The mean flow velocity also produces a significant effect on the performance of a straight-through resonator. For a short resonator, the increase in mean flow velocity will reduce the transmission loss of the main peak markedly but the corresponding frequency is virtually unaffected. The increase in mean flow velocity also eliminates the sharp main noise reduction peak for a long resonator. However, the transmission loss is increased markedly for frequencies below the peak frequency. Finally, it is noted that the results for a resonator with mean flow have to be verified by further experiments.

ACKNOWLEDGMENT

The work in this paper was supported by the National Science Council, Republic of China, under grant no. NSC 87-2611-E-002-045.

REFERENCES

1. D. D. Davis, G. M. Stokes and G. L. Stevens 1954 *NACA Report No*. 1192. Washington, DC: National Advisory Committee for Aeronautics. Theoretical and experimental investigation of mufflers with comments on engine-exhaust muffler design.
2. J. W. Sullivan and M. J. Crocker 1978 *Journal of the Acoustical Society of America* **64**, 207–215. Analysis of concentric-tube resonators having unpartitioned cavities.
3. J. W. Sullivan 1979 *Journal of the Acoustical Society of America* **66**, 772–788. A method for modeling perforated tube muffler component, I. theory, II. Application.
4. K. Jayaraman and K. Yam 1981 *Journal of the Acoustical Society of America* **69**, 390–396. Decoupling approach to modeling perforated tube muffler component.
5. P. T. Thawani and K. Jayaraman 1983 *Journal of the Acoustical Society of America* **73**, 1387–1389. Modeling and application of straight-through resonator.
6. M. L. Munjal, K. N. Rao and A. D. Sahasrabudhe 1987 *Journal of Sound and Vibration* **114**, 173–188. Aeroacoustic analysis of perforated muffler components.
7. K. S. Peat 1988 *Journal of Sound and Vibration* **123**, 199–212. A numerical decoupling analysis of perforated pipe silencer elements.
8. C. N. Wang, C. C. Tse and Y. N. Chen 1993 *Engineering Analysis with Boundary Elements* **12**, 21–27. A boundary element analysis of a concentric-tube resonator.
9. J. W. Sullivan 1984 *Journal of the Acoustical Society of America* **76**, 479–484. Some gas flow and acoustic pressure measurements inside a concentric-tube resonator.
10. T. W. Wu and L. Lee 1994 *Journal of Sound and Vibration* **175**, 51–63. A direct boundary integral formulation for acoustic radiation in subsonic uniform flow.
11. C. N. Wang, C. C. Tse and Y. N. Chen 1993 *Applied Acoustics* **40**, 91–106. Analysis of three dimensional muffler with boundary element method.
12. M. L. Munjal 1987 *Acoustics of Ducts and Mufflers*. New York: Wiley-Interscience.
13. K. N. Rao 1984 *Ph.D. thesis*, *Indian Institute of Science*, *Bangalore*, *India*. Prediction and verification of the aeroacoustic performance of perforated-element mufflers.